



Original scientific paper

Influence of reduction conditions of NiO on its mechanical and electrical properties

Yehor Brodnikovskiy[✉], Bogdan Vasylyv*, Viktoriya Podhurska*,
Mariusz Andrzejczuk**, Nikkia McDonald***, Oleksandr Kyrpa, Orest Ostash*,
Oleksandr Vasylyev, Robert Steinberger-Wilckens***, Malgorzata Lewandowska**

Frantsevich Institute for Problems of Materials Science, 3 Krzhyzhanovsky Str., Kyiv, 03680, Ukraine

**Karpenko Physico-Mechanical Institute, 5, Naukova Str., Lviv, 79060, Ukraine*

***Warsaw University of Technology, Faculty of Materials Science and Engineering, Wołoska Str.,
141, 02-507 Warsaw, Poland*

****Centre for Fuel Cell and Hydrogen Research, School of Chemical Engineering, University of
Birmingham, Birmingham, B15 2TT, United Kingdom*

[✉]Corresponding Author: bregor@ukr.net; Tel.: +380-44-424-0294; Fax: +1-111-111-112

Received: September 16, 2015; Revised: December 10, 2015; Accepted: February 10, 2016

Abstract

Yttria stabilized zirconia with a nickel catalyst (Ni-YSZ) is the most developed, widely used cermet anode for manufacturing Solid Oxide Fuel Cells (SOFCs). Its electro-catalytic properties, mechanical durability and performance stability in hydrogen-rich environments makes it the state of the art fuel electrode for SOFCs. During the reduction stage in initial SOFC operation, the virgin anode material, a NiO-YSZ mixture, is reduced to Ni-YSZ. The volume decrease associated with the change from NiO-YSZ to Ni-YSZ creates voids and causes structural changes, which can influence the physical properties of the anode. In this work, the structural, mechanical and electrical properties of NiO samples before and after reduction in pure H₂ and a mixture of 5 vol. % H₂-Ar were studied. The NiO to Ni phase transformations that occur in the anode under reducing and Reduction-Oxidation (RedOx) cycling conditions and the impact on cell microstructure, strength and electrical conductivity have been examined. Results show that the RedOx treatment of the NiO samples influence on their properties controversially, due to structural transformation (formation of large amount of fine pores) of the reduced Ni. It strengthened the treated samples yielding the highest mechanical strength values of 25.7 MPa, but from another side it is resulting in lowest electrical conductivity value of $1.9 \times 10^5 \text{ S m}^{-1}$ among all reduced samples. The results of this investigation shows that reduction conditions of NiO is a powerful tool for influence on properties of the anode substrate.

Keywords

NiO, Ni, RedOx, SOFC anode

Introduction

Solid Oxide Fuel Cells (SOFCs) are energy conversion devices that convert chemical energy into electrical energy with higher conversion efficiencies and lower greenhouse gas emissions than conventional heat engines [1]. Traditional materials used in the manufacture of SOFCs include Ni-YSZ cermet for the anode, YSZ (8-10 mol. % Ytria Stabilized Zirconia) for the electrolyte and LSM-YSZ (Lanthanum Strontium Manganite – YSZ composite) for the cathode. These SOFCs typically operate on H₂ at temperatures of 700-850 °C. Literature delivers vast information regarding SOFC component requirements [1]. Since this paper discusses research centered on anode material properties, anode component requirements will be the main focus. Ni has proven to be the best material for use in SOFC anodes due to its high catalytic activity for hydrogen oxidation, absence of undesirable chemical interactions with YSZ and good electronic conductivity, making Ni-YSZ the anode material of choice [2]. For simplification of anode manufacturing, NiO powder is typically used instead of Ni metal as Ni metal melts at temperatures commonly used for cell sintering. Because NiO does not form solid solutions with YSZ, the NiO-YSZ composite is reduced to a Ni-YSZ cermet during cell operation [3].

The reduction kinetics of NiO powders have been thoroughly studied [4-5], also it is known that the reduction of NiO to Ni is accompanied by volume and structural changes which influence the physical and mechanical properties of the anode [6-8]. It is clear that the transformation of NiO to Ni during reduction brings the changes into the anode structure and determines its final properties. To understand the impact of Ni phase transformations during reduction on the creation of Ni-metal networks within the anode composite the study of NiO properties after reduction are required. Moreover, normal SOFC start-up/shut down procedures where fuel flow is interrupted and system temperature is reduced may result in oxidation and reduction of Ni, which further greatly influences anode microstructure. This process, commonly referred to as RedOx cycling, is considered unfavorable by some researchers [8] due to drastic volume changes of the Ni phase, cracking and reduced strength of anode. While other researchers show RedOx cycling improves anode electrical and mechanical properties [9], at least initially. There is insufficient data to determine whether RedOx cycling improves or impairs the physical properties (electrical conductivity, mechanical strength) of Ni-YSZ anodes. To develop a better understanding of the influence of nickel phase on structure formation and properties of SOFC anode, it is important to study the microstructural changes of NiO samples and their properties before and after reduction and RedOx cycling. This work continues the previous study [10] and represents more details concerning formation of NiO structure under variable reduction conditions. The relationships between mechanical, electrical properties of treated NiO and its structure were established.

Experimental

In this study commercial NiO powder (d₅₀ = ~300 nm, Donetsk Chemical Reagent Plant, Ukraine) was used. The NiO powder was wet ball milled in alcohol using ZrO₂ media balls for 24 h and left to dry in air. The powder was passed through a 100 mesh sieve to achieve homogeneity and a narrow particle size distribution. Chromatographic thermal desorption (Sorbometr P2, N₂ - gas adsorbate, Ar – gas carrier) and laser granulometry (SK Laser Micron Sizer PRO-7000) studies were carried out to determine powder surface area and agglomerate sizes. The size of the initial particles (crystallites) was estimated from TEM images of the powder. Reduction and RedOx cycling studies were performed on 25 mm diameter and 1.5-2 mm thick disc shaped samples that were pressed uniaxially at 20 MPa and then sintered at 1400 °C for 2 h in air using a VMK 1600

Linn High Therm furnace (Germany). To improve compaction of as-pressed samples, polyvinyl alcohol was used as a plasticizer. The porosity of the sintered NiO samples was measured by means of the Archimedes method.

All NiO samples were divided into three groups and their reduction was carried out under three different testing conditions. The first group was reduced by holding the samples in high purity hydrogen (99.99 vol. % H₂) at 600 °C for 4h. The second group was reduced by holding the samples in a 5 vol. % H₂-Ar fuel mixture at 600 °C for 4h and the last group was exposed to 5 RedOx cycles. Each RedOx cycle consisted of an initial 1h dwell at 600°C in the 5 vol. % H₂-Ar fuel mixture followed by a 1 h dwell at 600 °C in air and ending with a 1h hold at 600 °C in the 5 vol. % H₂-Ar fuel mixture [9]. 600 °C for the reduction of NiO samples was chosen as temperatures above 600°C can promote not only the sintering of a reduced highly porous Ni-metal layer but also decrease the kinetics of the reduction process due to mass transfer limitations [5]. It was shown that temperatures within the 550-600 °C range are most effective for the reduction of NiO powders and that the reduction of NiO compacts at 600 °C preserves the newly formed pores inside the Ni-grains.

Resistance measurements of the reduced samples were obtained by employing the DC 4-pt probe lateral method in air at 25°C. Mechanical strength tests for the non-reduced and reduced samples were performed by using the ring-on-ring biaxial bending method at room temperature [11].

Micrographs of the NiO grain shape and size were obtained using a TEM JEM100CXII, the cross-sectional microstructures of the reduced and non-reduced NiO samples were compared using a Superprobe 733 SEM (JEOL, Japan), and a high-resolution NB5000 dual-beam system microscope (Hitachi High Technologies Corporation, Japan) was used for internal structure characterization. 3D image analysis of the treated NiO was carried out using focused ion beam (FIB-SEM) microscopy. NiO porosity and post-reduction volume phase changes were calculated via estimation of surface area of different NiO phases contained within the SEM sample images by means of GIMP and ImageJ software.

Results and discussion

Powder characterization

A summary of the characterized NiO powder is presented in Table 1. It can be seen that the powder has a low surface area of 3 m² g⁻¹ and consists of big agglomerates with an average size of 12.9 μm. Figure 1 represents the general view of the initial particles of the NiO powder. NiO samples made from this powder were highly porous with an average porosity of 40 ± 4 %.

Table 1. Properties of NiO powder.

Initial particles size, nm	Agglomerate size, μm	specific surface area, m ² g ⁻¹
100-150	12.9	3

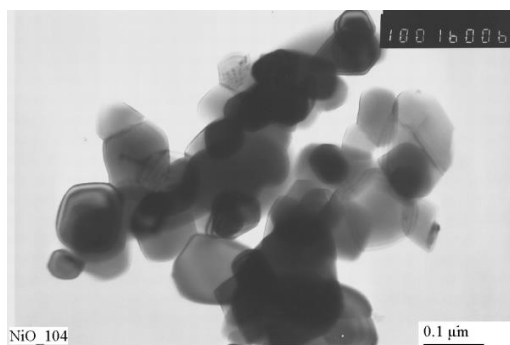


Figure 1. TEM image of NiO powder

Microstructure

The microstructure of the NiO samples in the non-reduced state is presented in Figure 2a. It can be seen that the sample consists of dense grains without visible defects along the boundaries and surfaces of the grains. The SEM image in Figure 2b shows a sample reduced in the 5-vol. % H₂-Ar mixture at 600 °C for 4 h which has fine pores along the grain boundaries and no visible changes in grain surfaces. It appears that the reduction of NiO in the 5 vol. % H₂-Ar mixture mostly effected on its grain boundaries. It is well known that the areas nearby grain contacts has the higher surface energy comparing to the grain surfaces what, for example, initiate diffusion processes and neck growth between grains during sintering of the powders compacts [12]. Thus, observed in Figure 2b structural changes of grain contacts can be explained by the aspiration of the material (NiO) to decrease its surface energy of the grain contacts via reduction of NiO to Ni. In other words, the grain boundary sites are more energy favored over grain surfaces for carrying out reduction processes. Also, it is known that the reduction of NiO in a hydrogen-containing medium begins from the nucleation of metallic clusters which then grow into crystallites at a near linear rate and this occurs at the interface between NiO and reduced porous Ni [4,5]. It means that the newly formed interface between NiO and reduced Ni is also more energy preferable site for further carrying out reduction processes comparing with the non-reduced NiO surface. Due to this, the primary reduction of the grain contacts results in further facilitation of the reduction front spreading in the direction from grains contacts to the grain cores due to already formed metallic Ni. This conclusion is in a good agreement with the FIB section of the reduced NiO samples in the 5 vol% H₂-Ar mixture pictured in Figure 3a, which reveals much reduced grain contacts compared with the grain surfaces. As can also be seen in Figure 3a, as in Figure 2b, the NiO grains were only partly reduced - the core remained unaffected. The SEM micrograph obtained in BSE mode (Figure 3a), created a contrast in the imaging allowing a clear distinction between the Ni and NiO phases. The thickness of an outer Ni-metal rim surrounding the NiO grains is less than 400 nm. From Figure 3a it is possible to estimate the specific area of the Ni-metal rim relative to the total area of the grains. This estimation indicates that the Ni-metal rim is 11 % of the whole NiO volume. Thus, only about 11 % of the NiO phase was reduced to Ni in a mixture of 5 vol. % H₂-Ar. The partial reduction of the NiO samples can be explained by insufficient contact between H₂ (reducing agent) and the NiO surface due to the low content of H₂ in the fuel and/or insufficient dwell time and/or too low operating temperature. These findings are in good agreement with the results of previous studies [13].

The detection of the reduction front nucleation and its spreading inside the grains of NiO helps to better understand the kinetics of the NiO reduction process. Nowadays, in order to explain the kinetics of the reduction process of NiO, the shrinking core model and the grain model employed by Szekely *et al.* [14,15] are generally used. The shrinking core model assumes that during reduction, the solid NiO particle consists of an un-reacted core (NiO), shelled by a uniform layer of the reaction product (Ni-metal rim). As the reaction proceeds, this layer thickens and the un-reacted core shrinks. In the grain model, a particle is considered an agglomerate of the individual grains. The reduction of such particles occurs as the reduction of individual grains, proceeding non-uniformly and causing reduction fronts to appear at different sites [4].

In the case of highly porous NiO samples, the presence of brachiate porous channels facilitates the reduction according to the grain model, following further clarification. Firstly, the appearance of the nucleation of the reduction front is not as random as the grain model suggests [4]. The

reduction begins from specific sites with the highest surface energy such as grain contacts. It is possible to assume that the activity of these sites can be estimated via the dihedral angle between two given grains in the same way as for a sintering process [12]. Secondly, the direction of the reduction front spreading from grain contacts to the grain cores is not observed as a gradual reduction of individual NiO grains uniformly from grain surfaces to the cores as suggested by the shrinking core model.

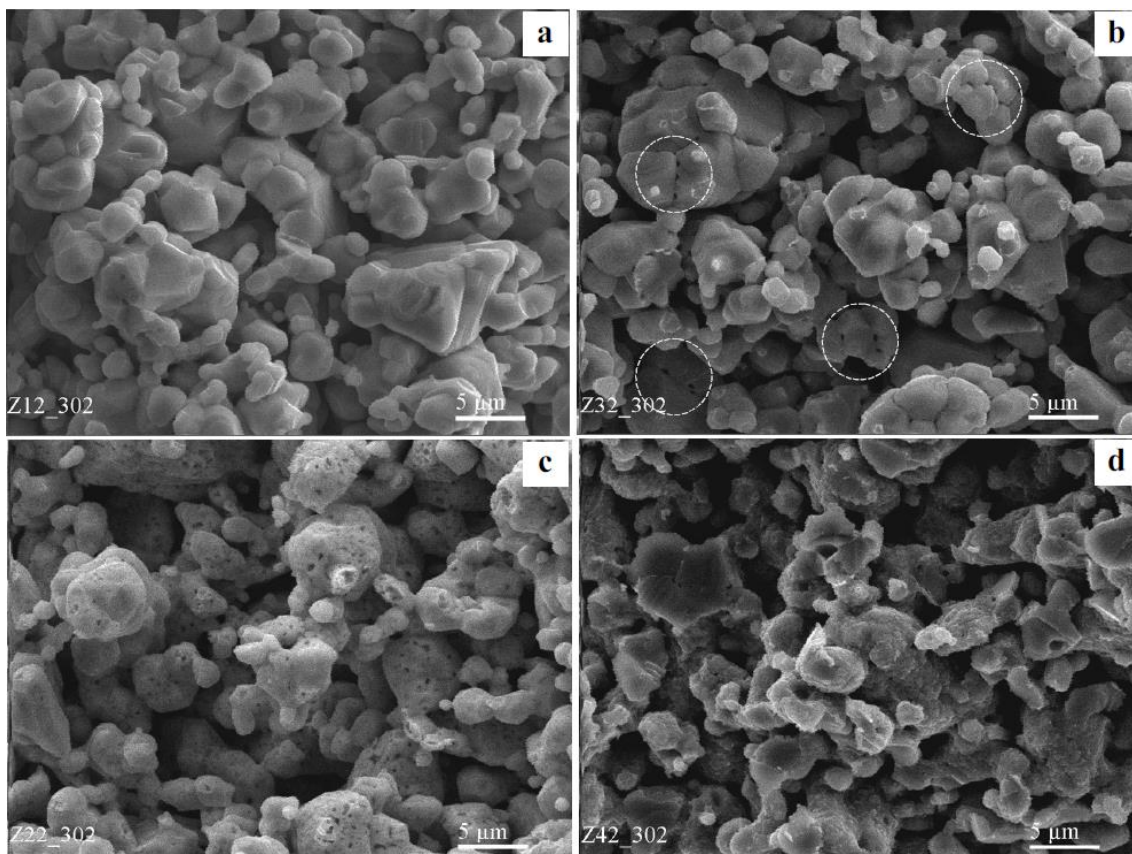


Figure 2. Typical SEM images of fracture surfaces of NiO samples before (a) and after reduction in different conditions: b – 5 vol. % H₂-Ar; c – pure H₂; d – RedOx

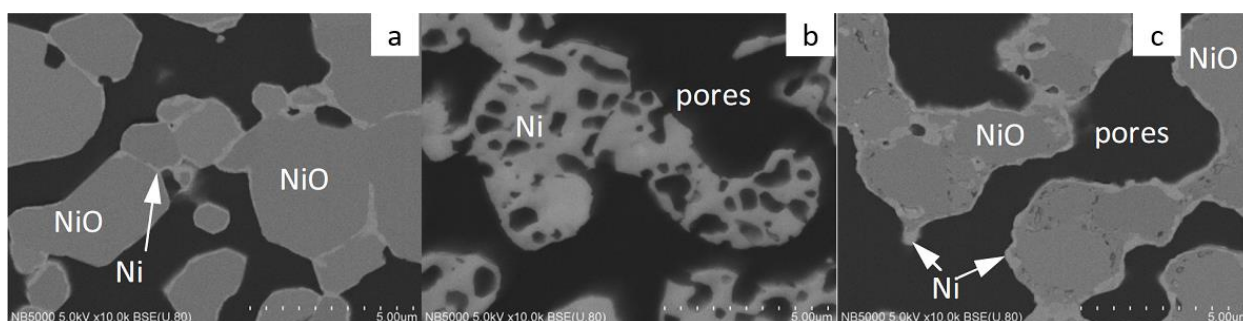


Figure 3. SEM images of NiO sample after (a) reduction in mixture 5 % H₂-Ar at 600 °C; (b) reduction in pure H₂ at 600 °C; (c) RedOx in mixture 5 vol. % H₂-Ar at 600 °C

The full conversion of NiO into Ni was achieved during reduction of the NiO samples in pure H₂. This leads to a change in the grain surface as it becomes pitted with holes as seen it in Fig. 2c. The observed pits are most likely caused by the volumetric change of NiO to Ni during reduction. Research shows [7], that under reducing conditions, the physical dimensions (size/shape) of the initial NiO particles essentially stay the same but the volume changes of NiO-Ni occur by means of

pore formation inside the particles. The FIB sections of the NiO samples reduced in pure H₂ at 600 °C reveal a sponge-like Ni structure with pore sizes in the range of 50 to 500 nm as presented in Figure 3b. These results are also in agreement with previously reported findings [7,13]. Correlating the specific area of the newly formed pores to the specific area of the grains could give an approximation of the apparent porosity of the post-reduced NiO samples. So, the volume of the inner pores is 30% relatively to the volume of the grains. The initial porosity of the samples was 40 % and the volume of NiO phase was 60%, accordingly. After reduction of NiO to Ni 30% of solid phase became the newly formed pores. This 30 % from the initial solid phase NiO is 18 % of additional porosity to the initial porosity value 40 %. Thus, the total porosity of NiO sample after its reduction in pure H₂ is about 58 %.

The use of the 5 vol. % H₂-Ar fuel mixture for the reduction of the NiO compacts was chosen to monitor the steps of the reduction process to better understand the kinetics of NiO reduction. While the use of the 5 vol. % H₂-Ar gas mixture is not effective for full reduction of NiO to Ni-metal, it is very useful for studying the microstructural changes in NiO during reduction. Thus, this gas mixture was used to study the influence of RedOx treatment on the properties of NiO samples. An initial view of the SEM images of the RedOx treated samples pictured in Figure 2d, show peculiar changes on the surface of the grains when compared against samples in the initial state and those reduced in the 5 vol. % H₂-Ar gas mixture as displayed in Figures 2a and b respectively. The edges of the grains became smooth while their surfaces became corrugated without the presence of big pitting holes as observed for samples reduced in pure H₂. More detailed analysis of the RedOx treated samples reveal the transformation of the grain's surface structure as pictured in Figure 3c. The formed Ni-metal rim contained a lot of fine pores and resembled a sponge-like structure, while the cores of grains remain unreduced. The thickness of the Ni-rim of the RedOx treated samples was thicker than what was observed in a single reduction in the 5 vol. % H₂-Ar gas mixture. From Figure 3c the specific area of the Ni-metal rim relatively to the total area of the grains was estimated. This estimation indicates that Ni-metal rim is 19 % of total grain area. This is practically twice as much than what was seen during a single reduction treatment in the 5 vol. % H₂-Ar gas mixture.

The appearance of a larger volume of reduced Ni-layer in NiO samples after RedOx treatment, which includes oxidation cycles, can be explained by the creation of a porous structure on the Ni layer surface. This finding suggests that following each reduction cycle more volume of material is reduced due to an increase in the available sample area because of the presence of pores created during RedOx cycles. Practically, the RedOx treatment actualizes the step by step reduction of NiO increasing the thickness and volume of the reduced Ni-layer. Moreover, comparing the structures of NiO samples pictured in Figures 3a and 3c makes it possible to observe the dynamics of the propagation of the reduction front. It is noticeable that the thickness of the reduced Ni-layer in a grains contact zone is thicker than the reduced Ni-layer from the surface of the pore. This shows that the reduction of NiO compacts occurs in regions where there is grain-to-grain contact and these sites are a priority zone for NiO reduction.

RedOx treatment has an even stronger influence on the formation of Ni-to-Ni intergranular contact than what has been observed during a single reduction in the 5 vol. % H₂-Ar gas mixture and pure H₂. The difference in contacting between NiO grains after RedOx treatment and a single reduction in H₂ is clearly seen in the SEM images of their surfaces pictured in Figures 4a and 4b respectively. In the case of a single reduction, the angularity of the grains are visible much like what is observed for unreduced NiO in Figure 2a but after RedOx treatment, the grains have

smoother edges yielding a more rounded shape which serves to expand the contact area between neighboring grains as observed in Figure 4b.

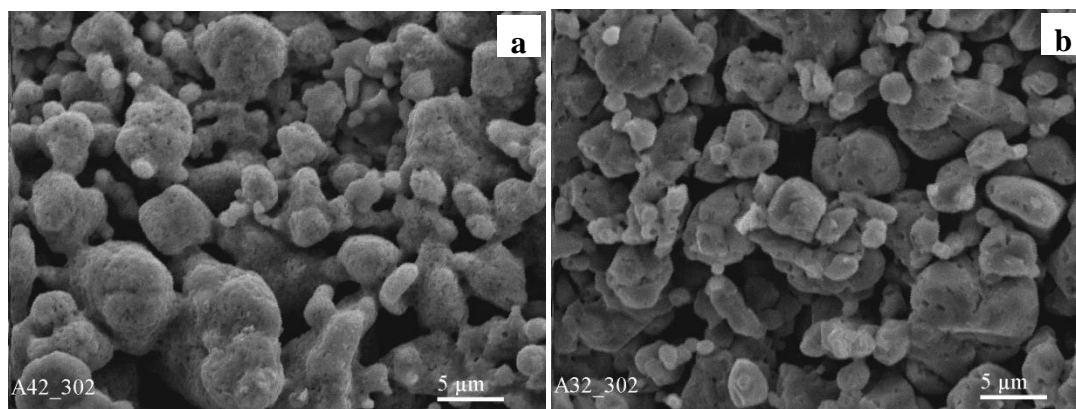


Figure 4. Typical SEM images of surfaces of NiO samples after RedOx treatment (a) and after single reduction in pure H₂ (b)

Mechanical strength

The results of this investigation on the mechanical strength of NiO samples before and after reduction in the aforementioned testing environments are summarized in Table 2. It can be seen that the mechanical strength of the samples increase after reduction and RedOx treatment when compared against the initial state.

Table 2. Properties of NiO samples after reduction in different conditions [10].

State of NiO samples	Strength, MPa	Electric conductivity, S m ⁻¹
Initial state	13.3	–
After reduction in 5 vol. % H ₂ -Ar	15.9	3.3·10 ⁵
After reduction in pure H ₂	18.8	2.7·10 ⁶
After RedOx treatment	25.7	1.9·10 ⁵

An increase in the mechanical strength of the 5 vol% H₂-Ar reduced samples (15.9 MPa) when compared against samples in their initial non-reduced state (13.3 MPa) can only be related to the formation of Ni-Ni grain contacts what was discussed in paragraph 3.2. The presence of the ductile Ni metal component in the grain contacts improved the strength of entire sample. When examining sample mechanical strength, it is clear that Ni-Ni contacting yields higher values than NiO-NiO contacting.

Despite the newly formed porosity (see paragraph 3.2), the strength (18.8 MPa) of the anode samples reduced in pure H₂ was also relatively higher than that in the initial state as indicated in Table 2. Such behavior can be explained by full transformation of NiO to Ni-metal and as result appearance of plasticity in the samples.

The strength of RedOx treated samples (25.7 MPa) is the highest compared with other samples. This obvious difference in strength can be explained by structural changes in the NiO samples after RedOx treatment. The newly formed fine porosity was observed in the Ni-rim of the RedOx treated samples as Figure 3c shows. It is seen that reduced grain contacts are very porous too. These fine pores complicate the passage of cracks through grain contacts and thus make them stronger. The close examination of the microstructure of the fracture surfaces picture in Figure 2 indicates the

cleavage facets only in RedOx treated samples (Figure 2d). The sizes of these facets are proportional to the sizes of the grains of the sample. This implies that the sample fracture permeates through the bodies of the non-reduced NiO grains. It is evident that formed porous Ni-Ni grain contacts are stronger over the dense NiO grain bodies (core).

Electrical conductivity

Depending on the selected reduction medium the NiO samples were reduced to a varying degree. The mixture of Ar with 5-vol. % H₂ can reduced NiO samples only partially. Only about 11 % of NiO was reduced to the Ni-metal as it was introduced above in paragraph 3.2. The grain surfaces and grain contacts were reduced to Ni-metal phase, but the grain cores left unreduced in NiO phase. NiO phase is a bad electronic conductor and limits the conductivity of the whole sample. Thus, only the reduced Ni-metal rim, a thin layer of the grain surfaces and grain contacts, can react as electronic conductor in this sample. Due to this, NiO samples reduced in the mixture 5 vol% H₂-Ar had relatively low electrical conductivity of $3.3 \cdot 10^5 \text{ S cm}^{-1}$ as listed in Table 2.

Despite of newly formed porosity during reduction and a quite high value of total porosity of 58% these samples had the highest electrical conductivity $2.7 \cdot 10^6 \text{ S cm}^{-1}$. This can be explained by the creation of the highest cross-sectional area of the conductor (Ni-metal) as a result of full transformation of the ceramic NiO sample into a Ni-metal sample.

For RedOx treatment, a mixture of 5 vol% H₂-Ar was used. Only partial reduction of NiO was observed in the treated samples. The reason is the same as in the case of single reduction of NiO in a mixture 5 vol% H₂-Ar. As introduced in paragraph 3.2 above, RedOx treatment allowed reducing more amount of NiO (about 19 %) when comparing with single reduction in a mixture – which was about 11 %. Due to the limitation of electronic conduction (Ni-metal phase) it was expected that these samples had much lower conductivity than the samples reduced in pure H₂, but they represented the lowest electrical conductivity of $1.9 \cdot 10^5 \text{ S m}^{-1}$ as listed in Table 2. In spite of the big difference in reduced Ni amount (practically double), a 42 % decrease in the electrical conductivity from $3.3 \cdot 10^5$ to $1.9 \cdot 10^5 \text{ S m}^{-1}$ for the NiO samples under RedOx treatment compared to the single gas mixture reduced samples was observed. This can be explained by newly formed fine porosity in the Ni-metal layer as seen in Figure 3c. Newly formed fine porosity as non-electronically conducting phase decreases the total conductivity of the Ni-rim due to thinning of the cross-sectional area of the conductor (Ni). In case of single reduction in the gas mixture the visible porosity in the Ni-rim was not observed as Figure 3a showed. Thus, a thin and dense Ni-rim formed after single reduction in gas mixture provides higher electrical conductivity compared with the thicker and highly porous Ni-rim formed after RedOx treatment.

Conclusion

Results show that the RedOx treatment of the NiO samples provides the formation of a large number of fine pores in the reduced Ni-metal layer. These newly formed fine pores influence on the properties of the NiO samples controversially. On one side, it strengthened intergranular contacts yielding the highest mechanical strength values of 25.7 MPa and, on the other side, resulted in the lowest electrical conductivity value of $1.9 \cdot 10^5 \text{ S m}^{-1}$ among all reduced samples.

The mechanical strength of the NiO samples after reduction in pure H₂ and 5 vol. % H₂-Ar were 18.8 and 15.9 MPa respectively, while the strength of NiO samples before reduction (initial state) was 13.3 MPa. The electrical conductivity of reduced NiO in 5 vol. % H₂-Ar ($3.3 \cdot 10^5 \text{ S m}^{-1}$) was

lower than the electrical conductivity of reduced NiO in pure H₂ ($2.7 \cdot 10^6 \text{ S m}^{-1}$) due to incomplete reduction of NiO.

These results demonstrate the large influence the reducing conditions have on the physical properties of the Ni-phase component of Ni-based anodes and, thus, the performance of SOFC cells. Reducing conditions in start-up of virgin cells and conditioning by careful choice of operating conditions and/or planned initiating RedOx cycles can greatly predefine cell performance.

It was also found that during reduction of the porous NiO samples, the nucleation of the reduction front begins in the intergranular contact zone and then spreads from there to the grain core. It was shown that this model of reduction front nucleation and spreading is more preferable than the assumption of uniform reduction as proposed in the shrinking core model. These results support the application of grain model NiO reduction kinetics for NiO agglomerates and improves the understanding of the behavior of reduction fronts throughout SOFC anodes.

Acknowledgments: *the authors are grateful to the European FP7 NANOMAT-EPC project "Deployment of Societally Beneficial Nano- and Material Technologies in European Partnership Countries" # 608906, the National Academy of Science of Ukraine, their projects "Hydrogen for alternative energetic and advanced technologies application" and "SOFC structural optimization based on consideration of interdiffusion at manufacturing and operation" for their respective support.*

References

- [1] N.Q. Minh, *Solid State Ionics* **174** (2004) 271 – 277.
- [2] A. Atkinson, S. Barnett, R. J. Gorte, J. T. S. Irvine, A.J. McEvoy, M. Mogensen, S.C. Singhal, J. Vohs, *Nature* **3** (2004) 17–27.
- [3] R.F. Martins, M.C. Brant, R.Z. Dominques, *Materials Research Bulletin* **4** (2009) 451–456
- [4] G. Plascenciaa, T. Utigard, *Chemical Engineering Science* **64** (2009) 3879–3888.
- [5] T. A. Utigard, M. Wu, G. Plascencia, T. Marin, *Chemical Engineering Science* **60** (2005) 2061 – 2068.
- [6] D. Sarantaridis, A. Atkinson, *Journal of Fuel Cells* **3** (2007) 246–258.
- [7] D. Waldbillig, A. Wood, D.G. Ivey, *Journal of Power Sources* **145** (2005) 206–215.
- [8] M. Ettler, H. Timmermann, J. Malzbender, A. Weber, N.H. Menzler, *Journal of Power Sources* **195** (2010) 5452–5467.
- [9] O. P. Ostash, B. D. Vasylyv, V. Podhurs'ka, O. D. Vasyly'ev, E. M. Brodnikovs'kyi, L. M. Ushkalov, *Journal of Materials Science* **46** (2011) 653–658.
- [10] V.Ya. Podhurs'ka, B.D. Vasylyv, O.P. Ostash O. D. Vasyly'ev, E. M. Brodnikovs'kyi, *Journal of Materials Science* **49** (2014) 805 – 811.
- [11] M. Radovic, E. Lara-Curzio, *Acta Materialia Journal* **52** (2004) 5747–5756.
- [12] F.F. Lange, *Journal of the European Ceramic Society* **28** (2008) 1509-1516.
- [13] M. Andrzejczuk, O. Vasylyev, I. Brodnikovskiy, V. Podhurska, B. Vasylyv, O. Ostash, M. Lewandowska, K.J. Kurzydłowski, *Materials Characterization* **87** (2014) 159-165.
- [14] V. J. Szekely, J. W. Evans, H. Y. Soh, *Gas Solid Reactions*, Academic Press, New York, USA, 1976, 372p.
- [15] J. Szekely, J. W. Evans, *Metallurgical Transactions*. **2** (1971) 1699-1710.